

BACH1, a Novel Helicase-like Protein, Interacts Directly with BRCA1 and Contributes to Its DNA Repair Function

Sharon B. Cantor,* Daphne W. Bell,†
Shridar Ganesan,* Elizabeth M. Kass,*
Ronny Drapkin,* Steven Grossman,*
Doke C.R. Wahrer,† Dennis C. Sgroi,‡
William S. Lane,§ Daniel A. Haber,†
and David M. Livingston*||

*The Dana-Farber Cancer Institute and the Harvard
Medical School

Boston, Massachusetts 02115

†Center for Cancer Risk Analysis and

‡Molecular Pathology Unit

Massachusetts General Hospital

Charlestown, Massachusetts 02129

§Microchemistry and Proteomics Analysis Facility

Harvard University

Cambridge, Massachusetts 02138

Summary

BRCA1 interacts in vivo with a novel protein, BACH1, a member of the DEAH helicase family. BACH1 binds directly to the BRCT repeats of BRCA1. A BACH1 derivative, bearing a mutation in a residue that was essential for catalytic function in other helicases, interfered with normal double-strand break repair in a manner that was dependent on its BRCA1 binding function. Thus, BACH1/BRCA1 complex formation contributes to a key BRCA1 activity. In addition, germline BACH1 mutations affecting the helicase domain were detected in two early-onset breast cancer patients and not in 200 matched controls. Thus, it is conceivable that, like BRCA1, BACH1 is a target of germline cancer-inducing mutations.

Introduction

Germline mutations in *BRCA1* lead to an increased lifetime risk of breast and/or ovarian cancer. The gene encodes an 1863 residue nuclear protein with an N-terminal RING and C-terminal BRCT domains. *BRCA1* contains little homology to known proteins. Evidence points to a role for this gene in the maintenance of genome integrity and in certain transcription regulation events (Deng and Brodie, 2000).

The C-terminal region of *BRCA1* contains two BRCT (*BRCA1* C-Terminal) motifs. These structures have been identified in many proteins engaged in genome integrity control (Koonin et al., 1996; Bork et al., 1997; Callebaut and Mornon, 1997) and, where studied, appear to participate in specific interactions with selected target proteins. For example, XRCC1 heterodimerizes with DNA ligase III in a base excision repair complex, and the BRCT motifs of both proteins are engaged in this interaction (Taylor et al., 1998).

For *BRCA1*, these motifs play a critical role in its ability

to mediate double-strand break repair and homologous recombination (Moynahan et al., 1999; Scully et al., 1999; Zhong et al., 1999; Wu et al., 2000). They also possess a transcription activation function (Chapman and Verma, 1996; Monteiro et al., 1996), which is abrogated by clinically relevant mutations. In keeping with the latter observations, the BRCT-containing region can interact with the RNA polymerase holoenzyme (Scully et al., 1997a) and with CtIP, a partner of the transcriptional corepressor, CtBP (Yu et al., 1998). However, the physiological significance of these two interactions is unknown.

In this regard, disease-associated mutations exist throughout *BRCA1*, but the majority of them result in a truncated product with loss of the extreme C terminus and one or both BRCT motifs (Breast Cancer Information Core (BIC)). Clinically relevant missense mutations exist within each BRCT motif, implying a link between their function and the execution of *BRCA1*-mediated tumor suppression. These findings notwithstanding, there is little biochemical understanding of how *BRCA1* functions as a tumor suppressor. Nonetheless, the evidence suggests that the genome integrity maintenance and the tumor suppression functions are linked (Welch et al., 2000).

In an effort to understand how the BRCT sequences function, we have screened for proteins that contact them directly. The search has led to the identification of BACH1, a novel member of the DEAH helicase family. From the results of a cell biological analysis and a clinical epidemiology study, it appears that BACH1 is a physiological partner of *BRCA1*, participating in the performance of both its DNA repair and its tumor suppressor functions.

Results

Screen for BRCT Binding Proteins

A GST fusion protein containing residues 1529–1863, which spans both BRCT motifs and extends to the *BRCA1* C terminus (GST-BRCT; Figure 1A), was generated. The modified GST moiety was labeled by in vitro phosphorylation with protein kinase A and used in far Western blotting experiments (Blancar and Rutter, 1992; Kaelin et al., 1992) where it detected four bands ranging from 50 to 220 kDa (whole-cell extract (WCE), Figure 1B). Among them was a protein of ~130 kDa, which was also detected in 293T and U2OS cell lysates (data not shown). This protein was also present in immunoprecipitates (IPs) generated with multiple *BRCA1* monoclonal antibodies (mAbs) (for an example, see Figure 1B, lane 3).

Binding of the 130 kDa band to the GST-BRCT probe was compromised when clinically relevant point mutant derivatives were used as the probe. One mutation [P1749R] led to greatly reduced binding and another [M1775R] (see Figure 1A) completely abolished binding of the 130 kDa protein (Figure 1C). Unlike their wild-type (wt) counterpart, the GST-BRCT mutant proteins also failed to interact with this polypeptide in solution (data not shown).

||To whom correspondence should be addressed (e-mail: david_livingston@dfci.harvard.edu).

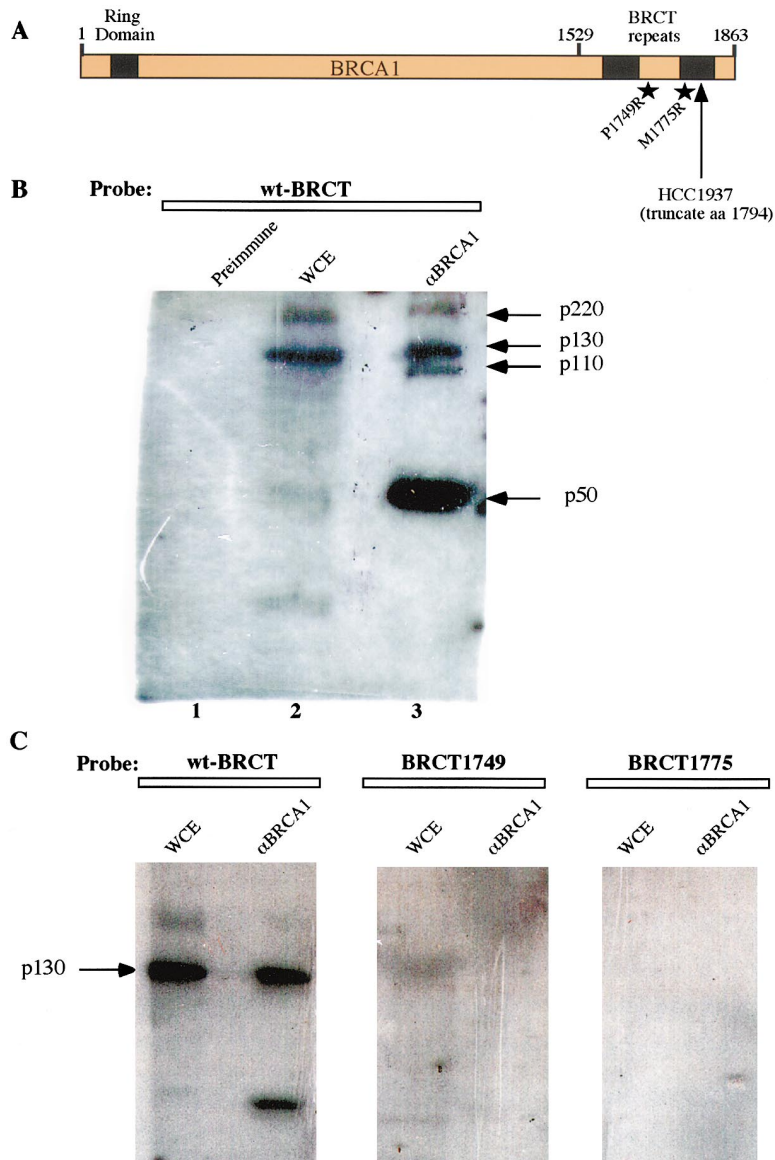


Figure 1. The BRCT Repeats of BRCA1 Interact with a Discrete Set of Polypeptides by Far Western Analysis

(A) Map of BRCA1 showing the BRCT motif-containing region (aa 1529–1863); this region also served as a probe in far Western analysis. Two different point mutations and the location of the BRCA1 truncation present in the HCC1937 cell line are noted with stars and an arrow, respectively.

(B and C) Far Western assays of HeLa whole-cell lysates (WCE) and of immunoprecipitates (BRCA1 preimmune rabbit and rabbit immune, c23 polyclonal Ab). (B) A 130 kDa band is present in a HeLa cell lysate and in an anti-BRCA1 immunoprecipitate when wt BRCT probe was used. (C) BRCT probes containing the mutations, P1749R or M1775R, failed to recognize the 130 kDa band.

Purification of the 130 kDa BRCA1 Binding Protein

To purify the 130 kDa protein, a GST-BRCT fusion protein bound to glutathione sepharose beads (GSSH) was incubated with HeLa cell nuclear extract. After extensive washing, proteins bound to the beads were eluted by boiling in SDS-containing buffer, electrophoresed on a polyacrylamide SDS gel, and stained with Coomassie blue (data not shown). When sufficient quantities of nuclear extract were immunoprecipitated, the 130 kDa band was readily detected by this approach. By contrast, it was not detected when either of the above noted BRCT mutant derivatives ([P1749R] or [M1775R]) was substituted for the wt BRCT fusion protein.

The 130 kDa band was excised from the gel and subjected to tryptic digestion within the gel material. The digest was eluted and subjected to microcapillary reverse phase HPLC and nanoelectrospray tandem mass spectrometry (MS/MS). The ensuing MS/MS spectra revealed that the 130 kDa protein sequence contains peptide sequences (see Experimental Procedures) encoded by three different EST sequences present on chromosome

17 (GenBank accession numbers AA397978, R16443, AI218496). Based on this information, a full-length cDNA was generated, as described in Experimental Procedures. The open reading frame of this clone predicts the synthesis of a 1249 residue polypeptide (Figure 2B). When this cDNA was transcribed and translated in vitro, its product comigrated with the endogenous 130 kDa protein and interacted with the wt GST-BRCT fusion protein, as described above (for an example, see Figure 4).

The N-terminal 888 residues of the protein reveal strong homology to the catalytic and nucleotide binding domains of known members of the DEAH helicase family. Among others, this group includes the xeroderma pigmentosum complementing group D (XPB) protein (Weber et al., 1990; Vermeulen et al., 1997; Coin and Egly, 1998) and human CHL1 (Amann et al., 1997; Figure 2C). The 130 kDa protein sequence contains the seven helicase-specific motifs that are conserved among members of the DEAH family. This helicase domain is 48% homologous to the human CHL1 protein. Like the other members of this family, the helicase domain in-

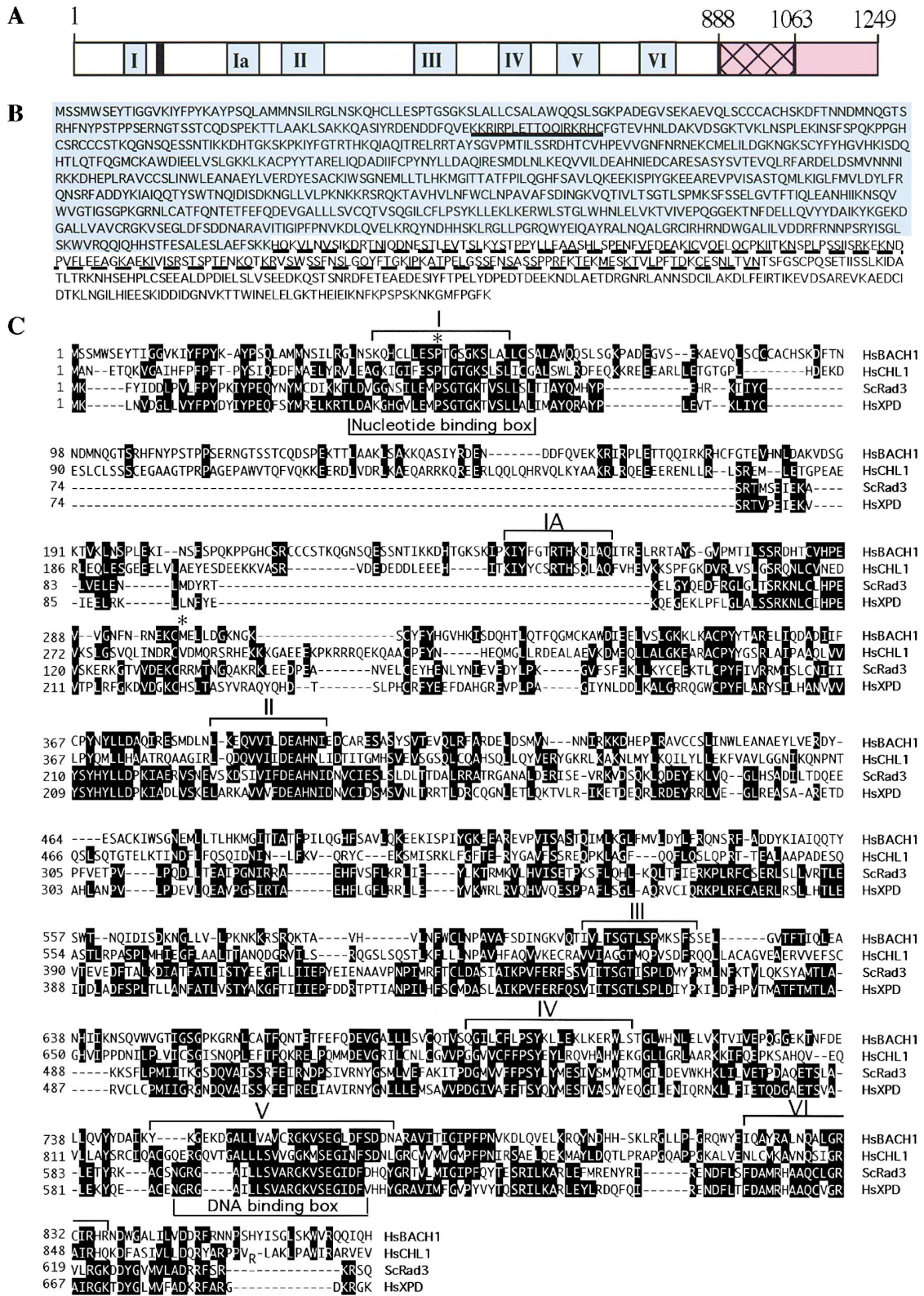


Figure 2. The BACH1 Sequence Is Significantly Homologous to that of DEAH Helicases
(A) DEAH helicase homology blocks are shown in roman numerals. The putative nuclear localization sequence (black rectangle) is shown. The helicase homology region of BACH1 spans residues 1–888. The BRCA1 binding domain spans residues 888–1063 (hatched box).
(B) The BACH1 amino acid sequence with its helicase homology region (1–888) (blue shaded region). The underlined, hatched area constitutes the BRCA1 binding domain, and the solid underlined region is predicted to contain a nuclear localization sequence.
(C) Homology alignment of the helicase domains of *Homo sapiens* BACH1 (HsBACH1), CHL1 (HsCHL1), and XPD (HsXPD), and *S. cerevisiae* Rad3 (ScRad3). Identical or similar amino acid residues are shaded. In addition, the seven conserved domains of known helicases are denoted above the sequence, and the nucleotide and DNA binding domains are shown below the alignment. BACH1 contains a canonical DEAH sequence in helicase box II. The (*) denotes the residues mutated in the cancer patients described in the text.

cludes a nuclear localization signal (Figure 2A). However, unlike other DEAH family members, the 130 kDa protein sequence contains a C-terminal extension of unknown function (Figure 2A). This particular sequence reveals 39% homology with synaptonemal complex protein 1, a major component of the transverse filaments of developing meiotic chromosomes (Schmekel et al., 1996).

Given the identical sequence properties of the gel-excised 130 kDa protein and the cloned polypeptide, their comigration in SDS gels, their ability to interact specifically with the BRCT-containing region of BRCA1, and the presence of a DEAH helicase domain, the 130 kDa protein was named BACH1 (for Brca1-Associated C-terminal Helicase). The *BACH1* gene was localized to chromosome 17q22 between markers D17S791 and D17S794, as defined by a Genemap 99 NCBI database search.

From a multiple-tissue cDNA panel (Clontech), BACH1 is ubiquitously expressed, with highest RNA levels in testis (data not shown). This expression pattern is similar to that reported for BRCA1, which is present at some level in all tissues but highest in testis (Miki et al., 1994; Zabludoff et al., 1996).

BACH1 Is a Nuclear Protein that Interacts with BRCA1 In Vivo

Monoclonal antibodies to BACH1 were raised against recombinant GST-BACH1 (residues 647–1043) and against a BACH1 C-terminal peptide (NFKPSPSKNKGMPFGFK). Western blots of extracts from three different human cell lines probed with these antibodies revealed the presence of intact BACH1 in all extracts (data not shown). Furthermore, anti-BRCA1 or anti-BACH1 IPs of extracts from asynchronously growing MCF7 cells, independently performed with two BRCA1 and two BACH1 mAbs, coprecipitated BRCA1 and BACH1 (Figure 3A). These data strongly suggest that BRCA1 and BACH1 interact in vivo. The BRCA1 RING domain-associated protein, BARD1, was also present in the IPs generated with BACH1 mAbs and vice versa (Figure 3A), suggesting that BACH1 exists in complex with both BRCA1 and BARD1.

Immunofluorescence analysis using BACH1 mAbs revealed the presence of punctate nuclear staining in multiple human cell lines. Focal BACH1 staining was detected in numerous, albeit not all, cells present in asynchronous cultures. BRCA1 nuclear dots, as noted previously, were detected in S and G2 phase cells (Scully et al., 1997c). In the majority of cells containing both types of nuclear foci, many of these structures colocalized with one another (Figure 3B). In synchronized cell populations, nearly complete colocalization of BACH1 and BRCA1 was detected in late S-G2 cells. Exposure to gamma irradiation or hydroxyurea did not affect the co-IP of BACH1 and BRCA1, and, like BRCA1, BACH1 underwent dynamic relocation to PCNA-containing structures after hydroxyurea exposure (data not shown) (Scully et al., 1997b).

In a line of BRCA1^{-/-} cells (HCC1937) that synthesize a mutant BRCA1 species with a truncated C-terminal region affecting the integrity of the second BRCT motif (Tomlinson et al., 1998) (see Figure 1A), this BRCA1 species and BACH1 failed to coimmunoprecipitate (Fig-

ure 3A). The abundance of BACH1 in these cells was reduced by comparison with that detected in MCF7 or 293T cells (data not shown). Correspondingly, although punctate BACH1 nuclear staining was detectable (Figure 3B, compare the lowermost middle panel with panel 2/lane 2), the intensity of the BACH1 nuclear dot pattern was lower in HCC1937 cells than in other cell lines containing intact BRCA1 (like MCF7) (Figure 3B). In keeping with these observations, when we used higher concentrations of BACH1 mAb in HCC1937, BACH1 foci were also readily detectable (data not shown).

When HCC1937 cells were reconstituted with full-length BRCA1 by recombinant retroviral infection (Scully et al., 1999), BRCA1/BACH1 complexes and costaining nuclear dots were again readily detected (Figures 3A and 3B), even though the intracellular abundance of BACH1 was unchanged (data not shown).

These findings complement the far Western blotting results showing that two intact BRCT repeat units of BRCA1 are essential for a stable BRCA1/BACH1 interaction. They further imply that the intensity of the BACH1 nuclear dot pattern is dependent, at least in part, upon the ability of BACH1 to interact with BRCA1. Taken together, the data indicate that BACH1/BRCA1 complex formation is accompanied by an enhancement of the BACH1 immunostaining signal and the appearance of a prominent BACH1 nuclear dot pattern. Moreover, BARD1, absent from anti-BACH1 IPs of HCC1937 lysates, reappeared in BACH1 IPs of BRCA1-reconstituted HCC1937 cells (Figure 3A). The coimmunoprecipitation data and immunostaining results suggest that BRCA1 and BACH1 interact in vivo. They also suggest that the BARD1/BACH1 interaction is indirect, relying upon the independent association of each protein with BRCA1.

BRCA1 Binds to a Segment of the BACH1 Carboxy-Terminal Region

To search for a region of BACH1 necessary for binding BRCA1, a series of deletion mutants of BACH1 were generated and S³⁵-labeled products were synthesized by in vitro translation. These polypeptides were each incubated with the wt GST-BRCT (1529–1863) fusion protein bound to GSSH beads, and binding of the relevant BACH1 species was examined after SDS gel electrophoresis and autoradiography (Figure 4). The data reveal that a discrete region of BACH1, C-terminal to the helicase domain and spanning residues 888–1063, is sufficient for BRCA1 binding (Figure 4).

Dominant Negative BACH1 Disrupts Double-Strand Break Repair

Having established that BACH1 associates with BRCA1 in vivo, we asked whether the interaction between BACH1 and the BRCT-containing region of BRCA1 contributes to BRCA1 function. BRCA1 plays a major role in the repair of double-strand DNA breaks (Moynahan et al., 1999; Scully et al., 1999; Snouwaert et al., 1999). Since BACH1 interacts with BRCA1 and belongs to the DEAH helicase family, some members of which have a role in DNA repair (Wood, 1999; Cleaver, 2000), we asked whether BACH1 plays a role in double-strand break repair (DSBR). Specifically, we asked whether overexpression of a BACH1 mutant leads to a defect in DSBR. A

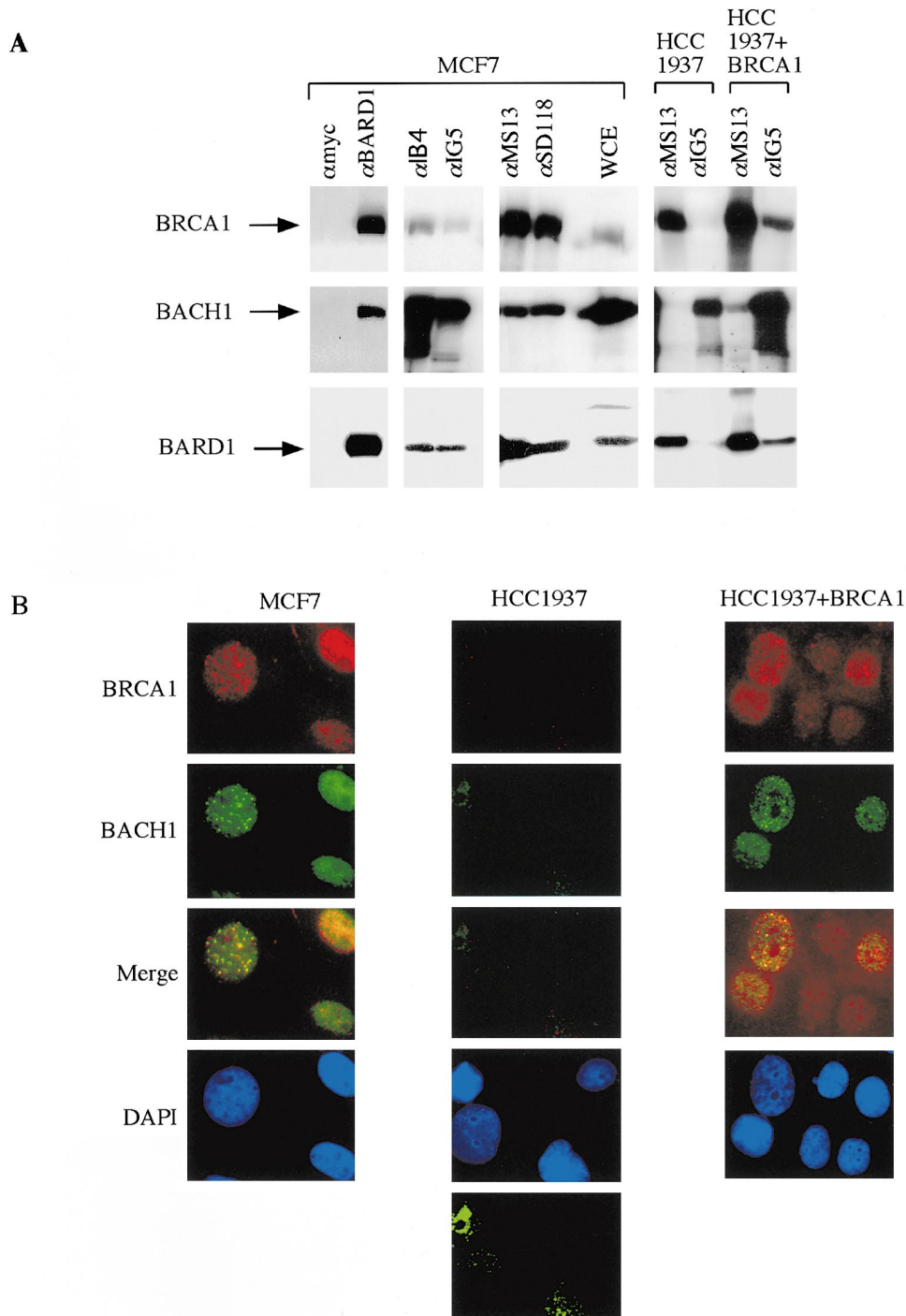


Figure 3. The BACH1/BRCA1 Interaction Depends on an Intact BRCA1 C-Terminal Region

(A) Immunoprecipitation/Western blot analyses of lysates of MCF7, HCC1937, and HCC1937 reconstituted with wt BRCA1. Immunoprecipitates, generated with the Abs denoted at the tops of the figures, were electrophoresed and blotted as described in Experimental Procedures. The blots were probed with α BRCA1 (MS110; upper third segment), α BACH1 (2G7; middle third segment), or α BARD1 (c20; bottom third segment). BACH1 was immunoprecipitated with either IB4 or IG5. BRCA1 was immunoprecipitated with either MS13 or SD118. In the first experiment (left panel), BARD1 immunoprecipitation was generated with c20 (α BARD1), and control precipitation was achieved with anti-myc monoclonal antibody. The data presented in the other panels are from a second experiment.

(B) BACH1 and BRCA1 colocalize in nuclear dots in MCF7 cells, and colocalization in HCC1937 cells requires reconstitution with wt BRCA1. Asynchronous MCF7 or HCC1937 $-/-$ BRCA1 cells were dually stained for BRCA1 (using affinity-purified, rabbit polyclonal antiserum to BRCA1, red) and BACH1 (using monoclonal antibody to BACH1, green), as described in Experimental Procedures. Significant colocalization of BRCA1 and BACH1 nuclear dots in a subpopulation of cells is reflected by the presence of yellow nuclear dots in the merged images. BACH1 immunostaining was readily detected in the same HCC1937 cells (lowest middle panel) that were originally analyzed in lane 2/panel 2 when the intensity of exposure of the latter image was increased. BACH1 nuclear dots were also readily detected when the BACH1 antibody concentration was increased 100-fold above that used in the other panels (data not shown).

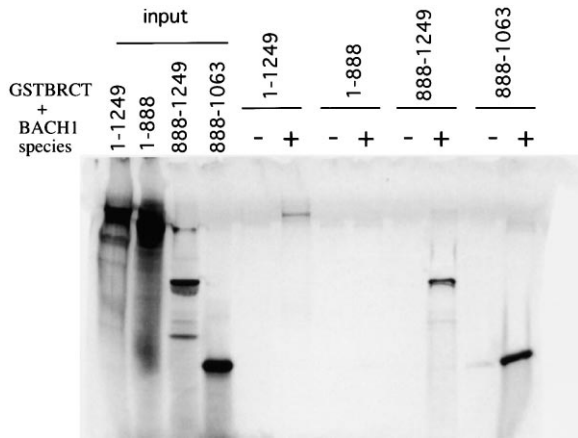


Figure 4. A Segment of the BACH1 C-Terminal Region Interacts with the BRCA1 BRCT Motifs

Various ³⁵S-labeled, in vitro translated BACH1 polypeptides were tested for binding to GST (-) or GST-BRCT:1529-1863 (+) fusion protein. Input lanes display 50% of the input of each in vitro translated BACH1 protein.

missense mutation that converts a lysine to an arginine was introduced at residue 52 (K52R). This residue is conserved in numerous ATPases and helicases, and has been shown to render the relevant protein incapable of hydrolyzing ATP (Sung et al., 1988; Ma et al., 1994). A double mutant, bearing both the K52R substitution and a second mutation ($\Delta C = \Delta$ l 888-1249) that eliminates the BRCA1 binding domain of BACH1 (K52R Δ C), was also generated.

To assess DSB repair in cells overproducing wt or mutant BACH1, U2OS cells were transiently cotransfected with a GFP-encoding vector and an expression vector encoding wt, K52R, or K52R/ Δ C BACH1. Transfected cultures were FACS sorted and the green fluorescing cells analyzed for expression of the relevant BACH1 species. Standardized Western blot analysis demonstrated comparable expression of the various proteins (Figure 5C). The sorted cells were either mock treated or gamma irradiated, and the abundance of double-strand breaks (DSB) in each culture was analyzed. Previous experience has shown that in multiple cell lines that synthesize wt BRCA1, there is nearly complete resolution of DSB by six hours after irradiation (Scully et al., 1999 and data not shown). Therefore, we analyzed DSB repair kinetics at 0, 3, and 6 hr following exposure to irradiation by pulsed field gel electrophoresis (Badie et al., 1995; Scully et al., 1999). As shown in Figure 5A, after exposure to 15 Gy, U2OS cells overproducing the K52R mutant of BACH1 displayed a marked delay in repair, as shown by an increase in the level of unrepaired breaks detectable at 3 and 6 hr. Importantly, cells synthesizing the double mutant, K52R/ Δ C, which should neither hydrolyze ATP nor bind BRCA1, revealed normal DSB repair capacity at all time points (Figure 5A). With these kinetics in mind, we also performed a statistical analysis of these effects, employing multiple experiments in which U2OS DSB repair was tested after transfecting the vector, alone, or vector encoding wt BACH1, K52R, or K52R/ Δ C BACH1. Statistically significant perturbation of repair

was detected following expression of the K52R mutant. By contrast, it was not observed in the presence of equivalent levels of either the wt or the double mutant protein. These results indicate that K52R perturbs DSB repair in a dominant negative fashion. They further show that this interfering effect is, in part, dependent on the ability of BACH1 to bind BRCA1. Therefore, BACH1, like BRCA1, appears to be important for DSB repair, and the BACH1/BRCA1 interaction contributes to the execution of this BRCA1-dependent function.

Analysis of BACH1 Sequence Variants in Sporadic and Familial Breast Cancer

Human genome analysis localized the *BACH1* gene to chromosome 17q22. This region is frequently targeted by allelic losses in sporadic breast cancer, and failure to detect *BRCA1* mutations in these cases has suggested the presence of an additional tumor suppressor gene in this segment (Callahan, 1998). Given the evidence linking BACH1 to proper BRCA1-mediated DSB repair and prior evidence suggesting a relationship between BRCA1-mediated DSB repair and its tumor suppression function (Scully et al., 1999), we initiated a search for mutations in 21 cell lines derived from sporadic breast and ovarian tumors. In addition, we screened the germline DNAs of 65 individuals with early-onset breast cancer, of whom 35 had a strong family history of breast and/or ovarian cancer but lacked mutations in either *BRCA1* or *BRCA2* (Table 1). Mutational analysis involved direct nucleotide sequencing of RT-PCR amplified *BACH1* cDNA. The template for each cDNA was mRNA isolated from an immortalized B cell line generated with the relevant patient's peripheral blood B cells. Mutation confirmation was performed by sequence analysis of the relevant, individual exons, amplified from genomic DNA.

Two heterozygous missense mutations were detected in the germlines of two breast cancer patients. The first mutation, identified in a young woman with breast cancer who had a strong family history of breast and ovarian cancer, resulted in a proline to alanine substitution at codon 47 (P47A). Unfortunately, germline DNA was not available from any of this patient's family members to test for cosegregation of the mutation with breast cancer in this kindred. However, the P47A mutation was not detected in the germline DNAs of 200 control individuals, indicating that it is unlikely to be a polymorphism in the population (<1/400 alleles), although other polymorphisms were identified (see Table 1). The second germline *BACH1* mutation, M299I, was also detected in a case of early-onset breast cancer and absent in 200 control individuals (Table 1). Both mutations reside within the region encompassing the helicase domain of BACH1. Indeed, the P47A mutation resides within a region resembling the highly conserved nucleotide binding box of known DEAH helicases, while the M299I mutation is positioned between two other boxed motifs (see Figure 2C). Given its location within a conserved box motif, we further investigated the P47A mutation.

Specifically, we incorporated this mutation into an otherwise wt *BACH1* allele and expressed both mutant and wt gene products in U2OS cells. Remarkably, despite comparable expression of the two transcripts (data not shown), the abundance of the mutant gene product

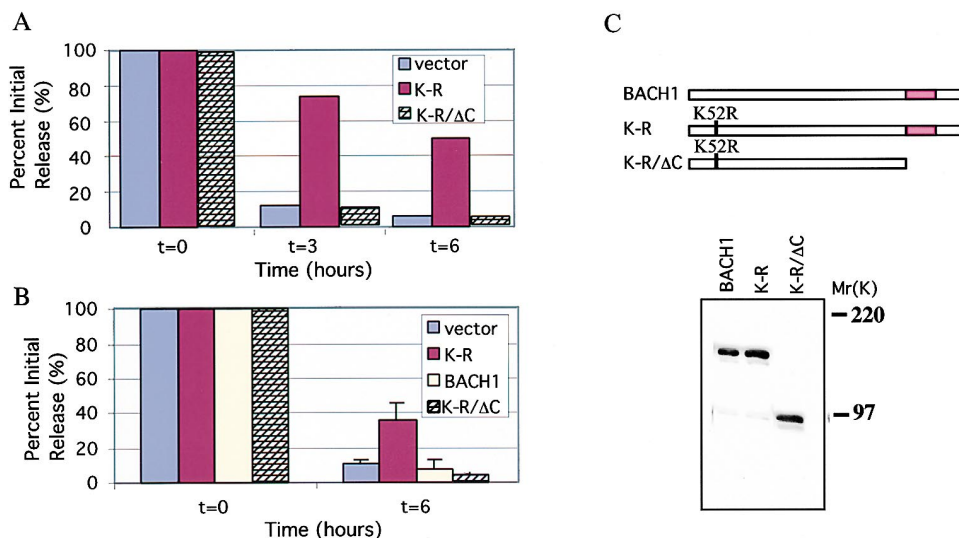


Figure 5. The BACH1 K52R Mutant Interferes with the Timely Repair of Double-Strand Breaks

(A) U2OS cells were transfected with a GFP-encoding vector and either K52R or K52RΔC, each expressed as a myc-6xhis-fusion protein. A control culture was transfected with vector alone. GFP-positive cells were FACS sorted and either exposed or not exposed to 15 Gy and harvested at the indicated times. Residual DSBs were determined by pulsed field electrophoresis as described in Experimental Procedures. Composite data analyzing results at three time points from two individual DSBR experiments are shown for K52R, K52RΔC, and vector. The data are the averages of 2–3 measurements at each time point.

(B) To further assess effects at the 6 hr time point, multiple experiments were performed using BACH1 (wt), K52R, K52RΔC, and vector alone, as described above. These data represent the mean and standard error of several independent experiments with at least 2–3 measurements per time point per experiment for each transfected culture.

(C) [Above], Maps of the primary structure of BACH1 (wt), K52R, and K52RΔC BACH1 are shown. [Below], FACS-sorted cells were lysed. Lysates were immunoprecipitated with myc antibody, and the relevant Western blot was probed with myc antibody. Western blot analysis showing that all three BACH1 proteins were expressed at the same level and were intact.

was considerably reduced, compared to the wt protein. To determine whether this was attributable to altered protein stability, the half-lives of the mutant and wt proteins were determined. Using the cycloheximide/chase method, the data indicated that BACH1 containing the P47A substitution was considerably less stable ($t_{1/2}$: ~ 1 hr) than either the wild-type protein ($t_{1/2}$: ~ 3 hr) or the K52R dominant negative mutant product ($t_{1/2}$: ~ 4 hr) (Figure 6). These results suggest that the P47A alteration constitutes a functionally significant mutation and suggest that reduced protein levels attributable to this mutant allele may be linked to breast cancer predisposition.

Analysis of a laser capture microdissected sample from this patient's tumor did not reveal homozygosity for the P47A change. However, prior fixation of the spec-

imen prevented screening of the full *BACH1* coding region for another mutation in the remaining allele or for any mutation that would restrict expression of the gene.

Discussion

Endogenous BACH1, a new member of the DEAH family of DNA helicases, interacts directly and specifically with the BRCT motif-containing domain of BRCA1. Moreover, BACH1 likely contributes to the DNA repair function of BRCA1, since a BACH1 derivative bearing a mutation in a key residue that is essential for catalytic function in other helicases interfered with normal DSBR in a manner that was dependent upon its ability to interact with BRCA1. Tumor-predisposing missense and deletion

Table 1. BACH1 Sequence Variations in Breast and Ovarian Cancer

Sequence Variant	Effect on Protein	Frequency				
		Familial Breast and Ovarian Cancer	Early-Onset Breast Cancer	Sporadic Breast Cancer	Sporadic Ovarian Cancer	Controls
C139G	PRO47ALA	1/35	0/30	0/13	0/8	0/200
G897A	MET299ILE	0/35	1/30	0/13	0/8	0/200
Polymorphisms						
G577A	VAL193ILE					3/200
C2755T	PRO919SER					11/21
G2637A	None					12/21
C3411T	None					10/23

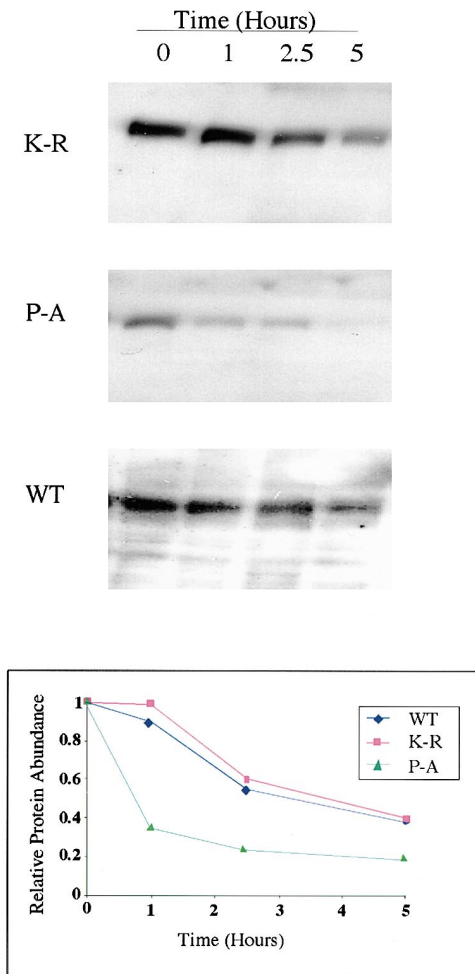


Figure 6. The BACH1 P47A Tumor-Associated Mutant Is Unstable Stability of wt and various mutant species of BACH1 was assessed by cycloheximide-chase analysis. BACH1 wt, K52R, and P47A were each expressed as a myc-6xhis-fusion protein in U2OS cells (10 μ g of each plasmid were transfected). Transfected cell lysates from each time point were immunoblotted for the c-myc epitope with 9E10 anti-myc Ab. The myc immunoblot was densitometrically scanned, and the intensity of each fusion protein band was plotted to determine the relevant half-lives. This experiment was repeated three times with similar results.

mutations in the BRCA1 BRCT domain, all of which render BRCA1 defective in its DSB repair function, also disrupted BACH1 binding to BRCA1. These data imply that BACH1 is integral to the role of BRCA1 in DSB repair.

Several lines of evidence suggest a role for BRCA1 in DSB repair. BRCA1 interacts with several proteins that are intimately involved in this process, including Rad51 and the Mre11/Rad50/Nbs-1 (MRN) complex (Scully et al., 1997b; Carney et al., 1998; Stewart et al., 1999; Zhong et al., 1999; Wang et al., 2000; Wu et al., 2000). Moreover, BRCA1-deficient cells reveal a chromosome breakage syndrome and defective DSB repair (Shen et al., 1998; Moy-nahan et al., 1999; Scully et al., 1999; Xu et al., 1999).

These findings notwithstanding, the mechanism by which BRCA1 participates in the DSB repair process remains unclear. Events that are likely to be intrinsic to the repair

process include the localized unwinding of DNA in the vicinity of a break. Enzymatic unwinding of DNA has already been shown to be an essential element in certain forms of DNA repair. For example, the XPD and XPB helicases associated with transcription-repair factor TFIIH are essential for nucleotide excision repair (reviewed in Coin and Egly, 1998), and this activity can be modulated by other proteins (Drapkin et al., 1994; Ohkuma and Roeder, 1994; Serizawa et al., 1994; Xiao et al., 1994; Wang et al., 1995; Qadri et al., 1996). In this context, the association of BRCA1 with a putative DNA helicase may help to shed light on the role of BRCA1 in the DSB repair process.

Similarly, it will be interesting to determine whether binding of BRCA1 affects the putative enzymatic function of BACH1. Alternatively, it is conceivable that BACH1 operates upstream of BRCA1, influencing the DSB repair-promoting function of the latter, or reciprocal BACH1 \leftrightarrow BRCA1 influence might exist after the creation of a DSB. What remains especially unclear is how and in what biochemical form the relevant influence is transmitted. Direct communication between a C-terminal segment of BACH1 and the BRCT motifs of BRCA1 would seem to be at least part of the story.

BRCA1 also functions in meiotic cells where it decorates the unsynapsed segments of developing synaptonemal complexes. In these regions, sister chromatids associate with one another in the presence of certain axial element proteins, BRCA1, BRCA2, Rad51, ATR, and other DNA replication/repair/checkpoint proteins (Keegan et al., 1996; Scully et al., 1997b; Chen et al., 1998; Yuan et al., 2000). Since the unsynapsed regions will eventually participate in appropriate pairing of homologous chromosomes, one or more proteins that are closely associated with them likely play(s) a role in the pairing/recombination process. Interestingly, the C-terminal region of BACH1 is homologous to SCP1 (Schmekel et al., 1996), an important component of the axial element, raising the question of whether BRCA1/BACH1 complexes may play a role in meiotic recombination.

The requirement for integrity of the BRCA1 BRCT motifs both for BACH1 binding and for BRCA1-mediated tumor suppression suggests a connection between these two functions. An association between loss of function of a helicase and either a decrease in cell viability or disease production is well established. The DEAH helicase family play significant roles in basal transcription, DNA repair, and chromosome transmission (reviewed in Hoeijmakers et al., 1996). In yeast, CHL1 appears to play a role in chromosome transmission, significant compromise of which can lead to nonviability. The *Saccharomyces cerevisiae* homolog of XPD, RAD3, is also essential for cell viability (Prakash and Prakash, 1989; Friedberg et al., 1995). In mammalian cells, XPD is part of TFIIH, which is required for both basal transcription and nucleotide excision repair (Weber et al., 1990; Drapkin et al., 1994; Coin and Egly, 1998). Nonlethal mutations of XPD are responsible for multiple genetic diseases including xeroderma pigmentosum, Cockayne Syndrome, and trichothiodystrophy (Coin and Egly, 1998). These examples highlight the diverse, yet key, roles played by members of the DEAH helicase family in biological processes dependent upon the mainte-

nance of proper DNA mechanics. They also underscore the close links that exist between abnormal/inadequate DNA mechanics and the emergence of disease.

In this context, it was interesting to detect an association between germline *BACH1* mutation and breast cancer development. In particular, two independent germline *BACH1* mutations were found among a cohort of 65 women with early-onset breast cancer, including one with a strong family history of breast and/or ovarian cancer but normal *BRCA1* and *BRCA2* genotypes. The mutation at proline 47, a highly conserved residue within the nucleotide binding domain of the DEAH family, is associated with *BACH1* protein destabilization. Thus, the P47A sequence change is most likely a loss-of-function mutation. While there is clearly no evidence indicating that mutation at *BACH1* is a common source of inherited breast cancer, the fact that *BACH1* mutations exist in certain early-onset breast cancer patients and not in 200 normal controls heightens speculation that, like the case of DSBR, *BACH1* activity is linked to *BRCA1* tumor-suppressing function. Of note, loss of heterozygosity (LOH) was not observed in cells from the tumor of the patient with a *BACH1* P47A germline mutation. However, inherent limitations in the method of analysis make it unclear whether or not the other *BACH1* allele is intact. If *BACH1* is intact, this would raise the question of whether heterozygosity at *BACH1* translates into haploinsufficiency. In such a case, somatic mutations in other genes might follow, with the subsequent mutation collection contributing to the emergence of a neoplastic phenotype in the relevant tumor cells.

The potential existence of a clinical association between a germline mutation in *BACH1* and early-onset breast cancer is intriguing and leads to speculation of a more general role for *BACH1* in cancer suppression. Unquestionably, broader epidemiological and formal human genetic analyses, as well as targeted mutation of the *Bach1* gene in the mouse, will be needed to address this possibility.

Experimental Procedures

Glutathione S-transferase (GST) Fusion Proteins

GST and GST fusion proteins were expressed in *E. coli* BLR (Novagen) transformed with pGEX2TK, pGST-BRCT, pGST-BRCT1749, or pGST-BRCT1775. Fusion proteins were purified by affinity chromatography using glutathione Sepharose beads (Pierce) as described (Kaelin et al., 1992). The relative protein concentration was estimated by Coomassie blue staining. Purified GST proteins were used in affinity/protein binding experiments (Chen et al., 1998) using either HeLa cell nuclear extracts or in vitro translated ³⁵S-labeled proteins. The latter were generated with the TNT system (Promega). Beads were extensively washed in NET-N buffer [150 mM NaCl, 0.5% NP-40, 20 mM Tris-HCl (pH8), 1 mM EDTA]. Bound proteins were separated by SDS-PAGE (10% gels) and/or visualized by autoradiography. For far Western blotting experiments, the pGEX2TK fusion proteins were labeled with ³²P-ATP as described (Amersham Pharmacia Biotech) and used as radioactive probes (Kaelin et al., 1992).

BACH1 Purification and Sequencing

Ten liters of HeLa cells, purchased from Cell Culture Science (Minneapolis, MN), were resuspended in low salt NET-N buffer. After a slow speed spin (1100 RPM), the pellet was lysed in 300 mM NaCl-containing NET-N buffer for 20 min on ice and then centrifuged at 15,000 RPM for 20 min. These supernatants were incubated with ~60 μl of packed glutathione agarose beads loaded with approximately 1 μg/μl of GST protein for 2 hr at 4°C. Following this preclear-

ing step, the supernatants were further incubated with ~60 μl of packed glutathione agarose beads loaded with approximately 20 μg of GST-BRCT fusion protein for 2 hr at 4°C. The beads were then collected by centrifugation and washed four times in NET-N containing 300 mM NaCl. Finally, the beads were boiled in SDS loading buffer containing 10% β-mercaptoethanol and analyzed by SDS-PAGE (10% gels). The gels were either stained or transferred to nitrocellulose (Schleicher & Schuell) and subjected to far Western blotting analysis. Where indicated, the 130 kDa *BACH1* band was visualized with Coomassie blue, excised from the gel, and subjected to sequence analysis.

Mass Spectrometry

The excised *BACH1* gel bands were subjected to reduction, carboxyamidomethylation, and tryptic digestion (Promega) within the relevant gel strips. Multiple peptide sequences were determined in a single run by microcapillary reverse phase chromatography directly coupled to an LCQ quadrupole ion trap mass spectrometer (Finnigan), equipped with a custom nanoelectrospray source. The column was packed in-house with 5 cm of C18 support into a one-piece 75 μm ID column terminating in a 15 μm tip (New Objective). Flow rate was 190 nl/min. The ion trap was programmed to acquire three successive scan modes consisting of: full scan MS over alternating ranges of 395–800 m/z and 800–1300 m/z, followed by two data-dependent scans on the most abundant ion in those full scans. These dependent scans allowed the automatic acquisition of a high resolution (zoom) scan to determine charge state, exact mass, and MS/MS spectra for peptide sequence information at <10 fmol. MS/MS spectra were acquired with a relative collision energy of 30%, an isolation width of 2.5 Da, and recurring ions were dynamically excluded. Interpretation of the resulting MS/MS spectra was facilitated by programs developed in the Harvard Microchemistry Facility (Chittum et al., 1998) and by database correlation with the algorithm SEQUEST (Eng et al., 1994). The following peptides were identified: TNFDELLQVYYDAIK, VSIGLDFSDDNAR, AVITIGIFPNVK, WLSTGLWHNLELVK, TVIVPEQGGEK, IDATLTR, TTWINELELGK, DLFEIR, ALN QALGR, QWYEIQAYR.

Immunoprecipitation, Immunoblotting, and Stability Analysis

Cultured cells were washed once with 10 mM sodium phosphate buffer (pH 7.4) containing 150 mM NaCl (PBS) and lysed in NET-N buffer. In a typical immunoprecipitation reaction, 100–300 μg of whole-cell extract was incubated with 1 μg of antibody and 20 μl of protein A Sepharose beads (1:1) at 4°C for 1–2 hr. Beads were washed four times in 1 ml of NET-N buffer. Proteins bound to the beads were eluted by boiling in SDS sample buffer, separated by SDS-PAGE, and transferred to nitrocellulose membranes (Schleicher & Schuell) using a semidry blotter (milliBlot-SDE system; Millipore). The membranes were used for far Western blotting (Kaelin et al., 1992) or for immunoblotting as described (Chen et al., 1998). Cycloheximide-chase experiments on transfected cells were performed as described (Maki and Howley, 1997).

Plasmids

Full-length *BACH1* cDNA was constructed from two phage containing partial cDNA fragments and a 5' RACE product generated as described by the manufacturer of the relevant kit (Gibco BRL). The fragments were digested and ligated together to produce a full-length *BACH1* sequence in a pBluescript II KS+/- vector (Stratagene). It was sequenced fully and found to be intact before use in experiments described here. To generate a mammalian expression plasmid encoding myc+ his-tagged full-length *BACH1*, the pBluescript vector containing wt *BACH1* cDNA was digested with NotI and ApaI to release the full-length *BACH1* sequence. The excised, full-length *BACH1* sequence was subcloned into the pCDNA3myc-6xhis vector (Invitrogen) to generate an in-frame polypeptide fused with the C-terminal myc-6xhis tag.

Sequences encoding truncated derivatives of *BACH1* were generated by PCR using the wt *BACH1* pBluescript vector as a template and the following primers: for the helicase domain derivative, [TTG CGGCCGCGCCACCATGGCACATTCATCAACTTGTCAGATT] and [TTG GGCCCGAAAATTAGCCCAAGGACTCCAG]; for the C-terminal domain-containing derivative, [TTGCGGCCGCGCCACCATGGATCCA

AAAAAGAAGAGAAAGGTATCCTTGGCTGAATTTTCCAAAAAG] and [AAGGGCCCTTAAAACCAGGAAACATGCCTTTATTTTGG]; and for the BRCA1 binding domain-containing derivative, [TTGCGGCCGCG CCACCATGGATCCAAAAAAGAGAGAAAGGTATCCTTGGCTGAA TTTTCCAAAAAG] and [AAGGGCCCTGTGTTTACTGTCAGATTTGA GGATTC].

These products were subcloned into a pCDNA3myc-6xhis vector (Invitrogen) in frame with the C-terminal myc-6xhis tag. To insure that the BACH1 C-terminal and BRCA1 binding domain fusion proteins localized to nuclei, an SV40 nuclear localization sequence was included in the 5' primer.

To inactivate the putative ATPase activity of BACH1, the lysine residue at position 52 was changed to an arginine, using a Quikchange site-directed mutagenesis kit (Stratagene). Two primers were used in this process: [CCACAGGAAGTGAAGGAGCTT AGCCTTAGCC] and [GGCTAAGGCTAAGCTCCTTCCACTTCTGT GGG]. To generate the (K52R Δ C) mutation, the helicase primers, listed above, were used with the (K52R) mutant BACH1 template. All newly generated recombinants were sequenced. To generate the tumor-associated mutant, the proline at position 47 was changed to an alanine by Quikchange site-directed mutagenesis (Stratagene) using the following primers: [CATTGTTTGTGGAGAGTGCCACA GGAAGTGGAAGGC] and [GCTTTTCCACTTCTGTGGCACTC CAACAAACAATG].

The BRCT-GST fusion protein was generated by PCR using the following primers: [ATCGGATCCATTAAGGTTGTTGATGTGGAG] and [AAGGATCCTCAGTAGTGTGGGGGATCTG]. The product was digested with BamHI/SalI and subcloned into pGEX2TK. The generation of M1775R and P1749R derivatives was carried out by standard PCR cloning techniques. Each derivative was verified by standard sequencing techniques. Templates containing these mutations were used with above-noted primers to introduce the BRCT1775 and BRCT1749 mutations into the pGEX2TK vector.

In Vitro Protein Binding Reactions

Expression plasmids encoding the full-length BACH1 and BACH1 polypeptides, generated as described above, were in vitro translated (TNT kit, Promega) and tested for binding to GST (-) or GST-BRCT:1529-1863 (+) fusion protein.

Cell Culture

U2OS and 293T cells were cultivated in Dulbecco's modified Eagle's medium (DMEM) containing 10% fetal calf serum (HyClone) at 37°C in a 10% CO₂-containing atmosphere. MCF7 cells were maintained in DMEM supplemented with 10% fetal bovine serum (HyClone). For transfection, a standard calcium phosphate precipitation method was used (Chen and Okayama, 1987). Cells were collected 48 hr after transfection.

Immunostaining

MCF7 cells were grown on coverslips, fixed with 3% paraformaldehyde/2% sucrose in PBS for 10 min., and permeabilized with 0.5% Triton X-100 as described previously (Scully et al., 1997c). Cells were then incubated with mouse monoclonal antibodies to BACH1 (2G7 or 1G5 at 1:50-1:100) and polyclonal anti-sera to BRCA1 (at 1:500) in PBS with 1% bovine serum albumin. After washing, appropriate species-specific, fluorochrome-conjugated secondary antibodies (Jackson ImmunoResearch Laboratories) were applied as recommended by the manufacturer, and fluorescence was visualized using a Nikon microscope.

Antibodies

Some of the anti-BRCA1 mAbs used were described previously (Scully et al., 1996; Chen et al., 1998). BARD1 antibody was made by subcloning a BgIII-XhoI fragment of BARD1 cDNA, encoding residues 201-777, into the BamHI-XhoI sites of pGEX-4T-1 to generate the vector for the expression of GST-BARD1 fusion protein. GST fusion protein purification, antibody production, and purification were performed as described previously (Scully et al., 1996; Chen et al., 1998). Two mouse monoclonal antibodies, generated against a specific BACH1 peptide (NFKPSPSKNKGMPGFK) (PP15-IB4 and PP112G7), and a third raised against GST-BACH1 (647-1043) (GO-IG5) were also used where indicated.

Double-Strand Break Repair Assay

Cells were cotransfected with BACH1 species and GFP, sorted after 24 hr by virtue of their GFP-associated fluorescence, and plated at 400,000 cells per 60 cm dish. 40 hr after transfection, the cells were either irradiated or mock irradiated and allowed to recover for various time points and then analyzed for their ability to perform DSBR, as described (Scully et al., 1999). Cells were irradiated with a 137 Cs source at 4°C and allowed to repair DNA breaks at 37°C. At the indicated times, cellular DNA was analyzed by pulse field gel electrophoresis as described (Badie et al., 1995). After electrophoresis, the gel was processed and stained with SYBR green as described (Kiltie and Ryan, 1997). Fluorescence was quantitated with a Molecular Dynamics Storm Scanner using the blue fluorescence channel and ImageQuant software (Molecular Dynamics). The fraction of DNA entering the gel was measured using the formula: Percent release = (signal in lane)/[(signal in lane) + (signal in plug)]/100. The quantity of signal present in unirradiated, parallel control cultures (<10% of total input DNA in a given lane) was taken as a measure of background signal and subtracted from the measured values. For kinetic studies, the data presented were normalized to the percent DNA released into the gel at T = 0.

Clinical Study Population

EBV-immortalized lymphoblastoid cell lines from 65 women diagnosed with breast cancer before the age of 40 were analyzed for BACH1 germline mutations. Sixteen cases had a definitive (3 or more affected individuals over 2 or more generations) family history of breast cancer, and 19 other individuals had a positive family history of breast-ovarian cancer. The remaining cases of early-onset breast cancer represent a subset of the general population at high risk for genetic predisposition. These individuals were part of a larger cohort of 408 women with early-onset breast cancer from Boston area hospitals (FitzGerald et al., 1996). Control EBV-immortalized lymphoblastoid cell lines were established from healthy blood donors registered in the blood banks of these hospitals. Both the early-onset breast cancer study group and the control population represent individuals within the Boston area. The two groups are well matched with respect to ethnicity as confirmed by equal contribution in the two populations of multiple polymorphic sequences. Thirteen sporadic breast cancer cell lines and 8 ovarian cancer cell lines were obtained from the American Type Culture Collection (Manassas, VA). They are: MDA-MB-415, MDA-MB-436, MDA-MB-453, MDA-MB-231, MDA-MB-157, MDA-MB-468, MDA-MB-435, MDA-MB-175, HS157, MCF7-ADR, HS275, T47D, BT549, OVCAR-3, OVCAR-4, OVCAR-5, OVCAR-8, OV1063, IGROV-1, MDA-2774.

Mutation Detection

Denaturing HPLC was used to detect mutations within the BACH1 coding region. Total mRNA was isolated using STAT-60 (Tel-test, Inc., Friendswood, TX). The entire BACH1 transcript was amplified in an RT-PCR reaction with primers BACH1-PRIM-F (GAATCGGAG CTCAGAGCGTTGCTTCG) and BACH1-PRIM-R (GGGCAACAGAC CAAGACTCTGTCTC) for 25 cycles at 95°C for 30 s, 58°C for 30 s, and 72°C for 4 min. Products of this reaction were diluted 100-fold and used as templates in subsequent nested PCR analyses to generate 14 overlapping fragments for dHPLC analysis. Primers and PCR conditions are available upon request. Wavemaker software (Transgenomic, Omaha, NE) and the Stanford prediction program (available at <http://insertion.stanford.edu/melt.html>) were used to predict the optimal temperatures for mutational analysis of each amplicon. Aberrant dHPLC profiles were confirmed by sequencing after reamplification of the fragment with primers that included M13-tailed primers. For sequencing analysis, PCR products were resolved by gel electrophoresis, treated with exonuclease I (Amersham Life Sciences) and with shrimp alkaline phosphatase (United States Biochemical). They were then diluted 6-fold prior to sequencing. Energy Transfer Dye Primer (Amersham Pharmacia Biotech) sequencing was performed according to the manufacturer's instructions. Potentially heterozygous nucleotides were marked and displayed for evaluation by Factura and Sequence Navigator (Applied Biosystems). Specifically, base positions at which the height of the secondary peak was >30% that of the primary peak were marked as heterozy-

gous and were confirmed by analysis of both sense and antisense strands. For LOH analysis, as reflected by the nature of the sequence at the codon responsible for residue 47, paraffin-embedded tumor blocks were sectioned and subjected to laser capture microdissection to isolate homogeneous regions of histologically normal cells and tumor cells. DNA was extracted using phenol-chloroform followed by ethanol precipitation. A genomic DNA fragment spanning codon 47 was amplified using forward (GATTAACAGCAAGCAA CATTGTTG) and reverse (CATGCTAAGCAGAACAAAGTAAGG) primers. PCR conditions consisted of: 35 cycles of 95°C for 30 s, 58°C for 30 s, 72°C for 30 s.

Acknowledgments

We are particularly grateful to all of our laboratory colleagues for helpful advice and discussions. We also wish to thank Jim DeCaprio for the preparation of BACH1 antibodies, Ralph Scully for the BRCA1 reconstituted HCC1937 cells, and Kerry Pierce for expert HPLC and mass spectrometry analysis. We also thank Junjie Chen for providing the BARD1 antibody. This work was supported by grants from the National Cancer Institute to D. M. L. and S. C. as well as a grant from the Dana Farber-Partners Gillette Women's Cancer Program and the Dana Farber/Harvard Specialized Program of Research Excellence (SPORE) in breast cancer from the National Cancer Institute (P50 CA89393). S. G. is a recipient of a Howard Hughes Medical Institute postdoctoral fellowship for physicians. R. D. is funded by NIH training grant T32 HL07627-16.

Received November 27, 2000; revised February 21, 2001.

References

Amann, J., Kidd, V.J., and Lahti, J.M. (1997). Characterization of putative human homologues of the yeast chromosome transmission fidelity gene. *CHL1*. *J. Biol. Chem.* **272**, 3823–3832.

Badie, C., Iliakis, G., Foray, N., Alsbeih, G., Cedervall, B., Chavaudra, N., Pantelias, G., Arlett, C., and Malaise, E.P. (1995). Induction and rejoining of DNA double-strand breaks and interphase chromosome breaks after exposure to X rays in one normal and two hypersensitive human fibroblast cell lines. *Radiat. Res.* **144**, 26–35.

Blanar, M.A., and Rutter, W.J. (1992). Interaction cloning: identification of a helix-loop-helix zipper protein that interacts with c-Fos. *Science* **256**, 1014–1018.

Bork, P., Hofmann, K., Bucher, P., Neuwald, A.F., Altschul, S.F., and Koonin, E.V. (1997). A superfamily of conserved domains in DNA damage-responsive cell cycle checkpoint proteins. *FASEB J.* **11**, 68–76.

Breast Cancer Information Core (BIC). http://www.nhgri.nih.gov/Intramural_research/Lab_transfer/Bic/.

Callahan, R. (1998). Somatic mutations that contribute to breast cancer. *Biochem. Soc. Symp.* **63**, 211–221.

Callebaut, I., and Morion, J.P. (1997). From BRCA1 to RAP1: a widespread BRCT module closely associated with DNA repair. *FEBS Lett.* **400**, 25–30.

Carney, J.P., Maser, R.S., Olivares, H., Davis, E.M., Le Beau, M., Yates, J.R., 3rd, Hays, L., Morgan, W.F., and Petrini, J.H. (1998). The hMre11/hRad50 protein complex and Nijmegen breakage syndrome: linkage of double-strand break repair to the cellular DNA damage response. *Cell* **93**, 477–486.

Chapman, M.S., and Verma, I.M. (1996). Transcriptional activation by BRCA1. *Nature* **382**, 678–679.

Chen, C., and Okayama, H. (1987). High-efficiency transformation of mammalian cells by plasmid DNA. *Mol. Cell. Biol.* **7**, 2745–2752.

Chen, J., Silver, D.P., Walpita, D., Cantor, S.B., Gazdar, A.F., Tomlinson, G., Couch, F.J., Weber, B.L., Ashley, T., Livingston, D.M., and Scully, R. (1998). Stable interaction between the products of the BRCA1 and BRCA2 tumor suppressor genes in mitotic and meiotic cells. *Mol. Cell* **2**, 317–328.

Chittum, H.S., Lane, W.S., Carlson, B.A., Roller, P.P., Lung, F.D., Lee, B.J., and Hatfield, D.L. (1998). Rabbit beta-globin is extended

beyond its UGA stop codon by multiple suppressions and translational reading gaps. *Biochemistry* **37**, 10866–10870.

Cleaver, J.E. (2000). Common pathways for ultraviolet skin carcinogenesis in the repair and replication defective groups of xeroderma pigmentosum. *J. Dermatol. Sci.* **23**, 1–11.

Coin, F., and Egly, J.M. (1998). Ten years of TFIIH. *Cold Spring Harb. Symp. Quant. Biol.* **63**, 105–110.

Deng, C.X., and Brodie, S.G. (2000). Roles of BRCA1 and its interacting proteins. *Bioessays* **22**, 728–737.

Drapkin, R., Reardon, J.T., Ansari, A., Huang, J.C., Zawel, L., Ahn, K., Sancar, A., and Reinberg, D. (1994). Dual role of TFIIH in DNA excision repair and in transcription by RNA polymerase II. *Nature* **368**, 769–772.

Eckner, R., Ewen, M.E., Newsome, D., Gerdes, M., DeCaprio, J.A., Lawrence, J.B., and Livingston, D.M. (1994). Molecular cloning and functional analysis of the adenovirus E1A-associated 300-kD protein (p300) reveals a protein with properties of a transcriptional adaptor. *Genes Dev.* **8**, 869–884.

Eng, J.K., McCormick, A.L., and Yates, J.R., III (1994). An approach to correlate tandem mass spectral data of peptides with amino acid sequences in a protein database. *J. Am. Soc. Mass Spectrom.* **5**, 976–989.

FitzGerald, M.G., MacDonald, D.J., Krainer, M., Hoover, I., O'Neil, E., Unsal, H., Silva-Arrieto, S., Finkelstein, D.M., Beer-Romero, P., Englert, C., et al. (1996). Germ-line BRCA1 mutations in Jewish and non-Jewish women with early-onset breast cancer. *N. Engl. J. Med.* **334**, 143–149.

Friedberg, E.C., Bardwell, A.J., Bardwell, L., Feaver, W.J., Kornberg, R.D., Svejstrup, J.Q., Tomkinson, A.E., and Wang, Z. (1995). Nucleotide excision repair in the yeast *Saccharomyces cerevisiae*: its relationship to specialized mitotic recombination and RNA polymerase II basal transcription. *Philos. Trans. R. Soc. Lond. B. Biol. Sci.* **347**, 63–68.

Hoeijmakers, J.H., Egly, J.M., and Vermeulen, W. (1996). TFIIH: a key component in multiple DNA transactions. *Curr. Opin. Genet. Dev.* **6**, 26–33.

Kaelin, W.G., Jr., Krek, W., Sellers, W.R., DeCaprio, J.A., Ajchenbaum, F., Fuchs, C.S., Chittenden, T., Li, Y., Farnham, P.J., Blanar, M.A., et al. (1992). Expression cloning of a cDNA encoding a retinoblastoma-binding protein with E2F-like properties. *Cell* **70**, 351–364.

Keegan, K.S., Holtzman, D.A., Plug, A.W., Christenson, E.R., Brainerd, E.E., Flaggs, G., Bentley, N.J., Taylor, E.M., Meyn, M.S., Moss, S.B., et al. (1996). The Atr and Atm protein kinases associate with different sites along meiotically pairing chromosomes. *Genes Dev.* **10**, 2423–2437.

Kiltie, A.E., and Ryan, A.J. (1997). SYBR green I staining of pulsed field agarose gels is a sensitive and inexpensive way of quantitating DNA double-strand breaks in mammalian cells. *Nucleic Acids Res.* **25**, 2945–2946.

Koonin, E.V., Altschul, S.F., and Bork, P. (1996). BRCA1 protein products. Functional motifs. *Nat. Genet.* **13**, 266–268.

Ma, L., Westbroek, A., Jochemsen, A.G., Weeda, G., Bosch, A., Bootsma, D., Hoeijmakers, J.H., and van der Eb, A.J. (1994). Mutational analysis of ERCC3, which is involved in DNA repair and transcription initiation: identification of domains essential for the DNA repair function. *Mol. Cell. Biol.* **14**, 4126–4134.

Maki, C.G., and Howley, P.M. (1997). Ubiquitination of p53 and p21 is differentially affected by ionizing and UV radiation. *Mol. Cell. Biol.* **17**, 355–363.

Miki, Y., Swenson, J., Shattuck-Eiden, D., Futreal, P.A., Harshman, K., Tavtigian, S., Liu, Q.Y., Cochran, C., Bennett, L.M., Ding, W., et al. (1994). A strong candidate for the breast and ovarian cancer susceptibility gene BRCA1. *Science* **266**, 66–71.

Monteiro, A.N., August, A., and Hanafusa, H. (1996). Evidence for a transcriptional activation function of BRCA1 C-terminal region. *Proc. Natl. Acad. Sci. USA* **93**, 13595–13599.

Moynahan, M.E., Chiu, J.W., Koller, B.H., and Jasin, M. (1999). Brca1 controls homology-directed DNA repair. *Mol. Cell* **4**, 511–518.

Ohkuma, Y., and Roeder, R.G. (1994). Regulation of TFIIH ATPase

- and kinase activities by TFIIIE during active initiation complex formation. *Nature* 368, 160–163.
- Prakash, L., and Prakash, S. (1989). Excision repair genes of *Saccharomyces cerevisiae*. *Ann. Ist. Super. Sanita* 25, 99–113.
- Qadri, I., Conaway, J.W., Conaway, R.C., Schaack, J., and Siddiqui, A. (1996). Hepatitis B virus transactivator protein, HBx, associates with the components of TFIIH and stimulates DNA helicase activity of TFIIH. *Proc. Natl. Acad. Sci. USA* 93, 10578–10583.
- Schmekel, K., Meuwissen, R.L., Dietrich, A.J., Vink, A.C., van Marle, J., van Veen, H., and Heyting, C. (1996). Organization of SCP1 protein molecules within synaptonemal complexes of the rat. *Exp. Cell Res.* 226, 20–30.
- Scully, R., Ganesan, S., Brown, M., De Caprio, J.A., Cannistra, S.A., Feunteun, J., Schnitt, S., Livingston, D.M. (1996). Location of BRCA1 in human breast and ovarian cancer cells. *Science* 272, 123–125.
- Scully, R., Anderson, S.F., Chao, D.M., Wei, W., Ye, L., Young, R.A., Livingston, D.M., and Parvin, J.D. (1997a). BRCA1 is a component of the RNA polymerase II holoenzyme. *Proc. Natl. Acad. Sci. USA* 94, 5605–5610.
- Scully, R., Chen, J., Plug, A., Xiao, Y., Weaver, D., Feunteun, J., Ashley, T., and Livingston, D.M. (1997b). Association of BRCA1 with Rad51 in mitotic and meiotic cells. *Cell* 88, 265–275.
- Scully, R., Chen, J., Ochs, R.L., Keegan, K., Hoekstra, M., Feunteun, J., and Livingston, D.M. (1997c). Dynamic changes of BRCA1 subnuclear location and phosphorylation state are initiated by DNA damage. *Cell* 90, 425–435.
- Scully, R., Ganesan, S., Vlasakova, K., Chen, J., Socolovsky, M., and Livingston, D.M. (1999). Genetic analysis of BRCA1 function in a defined tumor cell line. *Mol. Cell* 4, 1093–1099.
- Serizawa, H., Conaway, J.W., and Conaway, R.C. (1994). An oligomeric form of the large subunit of transcription factor (TF) IIE activates phosphorylation of the RNA polymerase II carboxyl-terminal domain by TFIIH. *JBC* 269, 20750–20756.
- Shen, X.-S., Weaver, Z., Xu, X., Li, C., Weinstein, M., Chen, L., Guan, X.-Y., Ried, T., and Deng, C.-X. (1998). A targeted disruption of the murine *Brca1* gene causes a γ -irradiation hypersensitivity and genetic instability. *Oncogene* 17, 3115–3124.
- Snouwaert, J.N., Gowen, L.C., Latour, A.M., Mohn, A.R., Xiao, A., DiBiase, L., and Koller, B.H. (1999). BRCA1 deficient embryonic stem cells display a decreased homologous recombination frequency and an increased frequency of non-homologous recombination that is corrected by expression of a *brca1* transgene. *Oncogene* 18, 7900–7907.
- Stewart, G.S., Maser, R.S., Stankovic, T., Bressan, D.A., Kaplan, M.I., Jaspers, N.G., Raams, A., Byrd, P.J., Petrini, J.H., and Taylor, A.M. (1999). The DNA double-strand break repair gene hMRE11 is mutated in individuals with an ataxia-telangiectasia-like disorder. *Cell* 99, 577–587.
- Sung, P., Higgins, D., Prakash, L., and Prakash, S. (1988). Mutation of lysine-48 to arginine in the yeast RAD3 protein abolishes its ATPase and DNA helicase activities but not the ability to bind ATP. *EMBO J.* 7, 3263–3269.
- Taylor, R.M., Wickstead, B., Cronin, S., and Caldecott, K.W. (1998). Role of a BRCT domain in the interaction of DNA ligase III- α with the DNA repair protein XRCC1. *Curr. Biol.* 8, 877–880.
- Tomlinson, G.E., Chen, T.T., Stastny, V.A., Virmani, A.K., Spillman, M.A., Tonk, V., Blum, J.L., Schneider, N.R., Wistuba, I.I., Shay, J.W., et al. (1998). Characterization of a breast cancer cell line derived from a germ-line BRCA1 mutation carrier. *Cancer Res.* 58, 3237–3242.
- Vermeulen, W., de Boer, J., Citterio, E., van Gool, A.J., van der Horst, G.T., Jaspers, N.G., de Laat, W.L., Sijbers, A.M., van der Spek, P.J., Sugawara, K., et al. (1997). Mammalian nucleotide excision repair and syndromes. *Biochem. Soc. Trans.* 25, 309–315.
- Wang, X.W., Yeh, H., Schaeffer, L., Roy, R., Moncollin, V., Egly, J.-M., Wang, Z., Friedberg, E.C., Evans, M.K., Taffe, B.G., et al. (1995). P53 modulation of TFIIH-associated nucleotide excision repair activity. *Nat. Genet.* 10, 188–195.
- Wang, Y., Cortez, D., Yazdi, P., Neff, N., Elledge, S.J., and Qin, J. (2000). BASC, a super complex of BRCA1-associated proteins involved in the recognition and repair of aberrant DNA structures. *Genes Dev.* 14, 927–939.
- Weber, C.A., Salazar, E.P., Stewart, S.A., and Thompson, L.H. (1990). ERCC2: cDNA cloning and molecular characterization of a human nucleotide excision repair gene with high homology to yeast RAD3. *EMBO J.* 9, 1437–1447.
- Welsh, P.L., Owens, K.N., and King, M.-C. (2000). Insights into the functions of BRCA1 and BRCA2. *Trends Genet.* 16, 69–74.
- Wood, R.D. (1999). DNA damage recognition during nucleotide excision repair in mammalian cells. *Biochimie* 81, 39–44.
- Wu, X., Petrini, J.H.J., Heine, W.F., Weaver, D.T., Livingston, D.M., and Chen, J. (2000). Independence of R/M/N focus formation and the presence of intact BRCA1. *Science* 289, 11a.
- Xiao, H., Pearson, A., Coulombe, B., Truant, R., Zhang, S., Regier, J., Triezenberg, S.J., Reinberg, D., Flores, O., Ingles, C.J., and Greenblatt, J. (1994). Binding of basal transcription factor TFIIH to the acidic activation domain of VP16 and p53. *Mol. Cell. Biol.* 14, 7013–7024.
- Xu, X., Weaver, Z., Linke, S.P., Li, C., Gotay, J., Wang, X.-W., Harris, C.C., Ried, T., and Deng, C.-X. (1999). Centrosome amplification and a defective G2-M cell cycle checkpoint induce genetic instability in BRCA1 exon 11 isoform-deficient cells. *Mol. Cell* 3, 389–395.
- Yu, X., Wu, L.C., Bowcock, A.M., Aronheim, A., and Baer, R. (1998). The C-terminal (BRCT) domains of BRCA1 interact in vivo with CtIP, a protein implicated in the CtBP pathway of transcriptional repression. *J. Biol. Chem.* 273, 25388–25392.
- Yuan, L., Liu, J.G., Zhao, J., Brundell, E., Daneholt, B., and Hoog, C. (2000). The murine SCP3 gene is required for synaptonemal complex assembly, chromosome synapsis, and male fertility. *Mol. Cell* 5, 73–83.
- Zabludoff, S.D., Wright, W.W., Harshman, K., and Wold, B.J. (1996). BRCA1 mRNA is expressed highly during meiosis and spermiogenesis but not during mitosis of male germ cells. *Oncogene* 13, 649–653.
- Zhong, Q., Chen, C.F., Li, S., Chen, Y., Wang, C.C., Xiao, J., Chen, P.L., Sharp, Z.D., and Lee, W.H. (1999). Association of BRCA1 with the hRad50-hMre11-p95 complex and the DNA damage response. *Science* 285, 747–750.

GenBank Accession Number

The GenBank accession number for the BACH1 sequence reported in this paper is AF360549.